

RESEARCH ARTICLE

Bivalves maintain repair when faced with chronically repeated mechanical stress

R. L. Crane^{*,‡} and M. W. Denny

ABSTRACT

Even though mollusks' capacity to repair shell damage is usually studied in response to a single event, their shells have to defend them against predatory and environmental threats throughout their potentially multi-decadal life. We measured whether and how mollusks respond to chronic mechanical stress. Once a week for 7 months, we compressed whole live California mussels (*Mytilus californianus*) for 15 cycles at ~55% of their predicted one-time breaking force, a treatment known to cause fatigue damage in shells. We found mussels repaired their shells. Shells of experimentally stressed mussels were just as strong at the end of the experiment as those of control mussels that had not been experimentally loaded, and they were more heavily patched internally. Additionally, stressed shells differed in morphology; they were heavier and thicker at the end of the experiment than control shells but they had increased less in width, resulting in a flatter, less domed shape. Finally, the chronic mechanical stress and repair came at a cost, with stressed mussels having higher mortality and less soft tissue than the control group. Although associated with significant cost, mussels' ability to maintain repair in response to ongoing mechanical stress may be vital to their survival in harsh and predator-filled environments.

KEY WORDS: Cyclic loading, Fatigue, Functional morphology, Mollusk, Mussel, *Mytilus californianus*

INTRODUCTION

Biomaterialized external armor, such as the shells of many mollusks, provides protection from predatory and environmental threats. Such encounters, if they do not kill an animal outright, can cause accumulating, weakening damage to its shell. Because mollusks do not periodically replace their shells (as arthropods do) and because damaging events occur repeatedly throughout an organism's potentially multi-decadal life, survival may depend on the capacity to continuously repair shell damage. However, expending resources to address such damage may come at a cost. How mollusks repair their shells and respond to chronic mechanical stress is a key parameter for understanding the success of their armor and ultimately their survival.

Mollusks have a remarkable ability to repair their shells, which has traditionally been studied experimentally in response to single damaging incidents. Studies of repair in response to punctured or clipped shells have provided insight into the timeline and

mechanisms of shell repair (Chen et al., 2019; Cho and Jeong, 2011; George et al., 2022; Meenakshi et al., 1973; Mount et al., 2004; Sleight et al., 2015), and studies inflicting one-time mechanical stress have demonstrated mechanical changes with shell repair (Crane et al., 2021; LaBarbera and Merz, 1992; O'Neill et al., 2018). However, these experimental manipulations do not address long-term changes or the repercussions of repeated encounters. Studies of scars on shells document survival and repair long after a damaging encounter and provide valuable ecological context (Blundon and Vermeij, 1983; Cadée, 1999; Harper et al., 2012; Peck et al., 2018), but these studies lack the rigorous controls of a laboratory experiment to isolate the capacity for ongoing repair and its long-term effects.

Studies of shell repair in response to a single damaging event do not account for the fact that shell damage has the potential to continuously accumulate in the field. Repeated mechanical stress can cause damage through the process of fatigue, in which microfractures accumulate and propagate through a material and decrease the force required for catastrophic failure (Mach et al., 2007; Suresh, 1998). Mollusk shells are susceptible to fatigue-caused weakening and breakage (Boulding and LaBarbera, 1986; Crane and Denny, 2020; Currey and Brear, 1984). Here, we tested the capacity of one mollusk species to maintain ongoing shell repair in response to fatigue damage using the intertidal California mussel, *Mytilus californianus*, as a study system. Its shell has a relatively tractable form: two domed valves joined by a hinge. Because of its ecological and economic importance, its general biology is well studied, and the mechanical properties of its shell are known (Crane and Denny, 2020).

We tested the capacity of the California mussel to repair its shell in response to ongoing mechanical stress; for 7 months, we compressed live mussels to a pre-determined subcritical force for 15 cycles, a treatment known to cause fatigue damage (Crane and Denny, 2020; Crane et al., 2021). We expected that they would be able to repair any accumulating damage to the shell, which would be evidenced by physical shell deposition and repair as well as maintenance of strength for shells of stressed mussels relative to that of a control group of mussels that did not experience the mechanical loading treatment. We further expected that experiencing weekly mechanical stress would trigger morphological changes associated with increasing shell strength. Finally, we expected that continuously investing in maintaining shell repair would come at some cost to the health and reproductive capacity of the mussels.

MATERIALS AND METHODS


Animal collection and experimental design

Mussels (*Mytilus californianus* Conrad 1837) ($N=195$; length mean \pm s.d.: 33 \pm 4 mm; range: 25–46 mm; length defined along anterior–posterior axis, see 'Morphological measurements', below) were collected at Hopkins Marine Station, Pacific Grove, CA, USA (Scientific Collecting Permit no. S-190720016-19072-001) from

Department of Biology, Stanford University, Stanford, CA 94305, USA.

^{*}Present Address: Department of Neurobiology, Physiology and Behavior, University of California, Davis, Davis, CA 95616, USA.

[‡]Author for correspondence (rlcrane@ucdavis.edu)

 R.L.C., 0000-0002-2438-4091; M.W.D., 0000-0003-0277-9022

one site (1.0–1.2 m above mean lower low water (MLLW), 36.62193°N, 121.90536°W). We did not include any mussels with significant damage to the periostracum or with external damage that revealed the nacreous layer.

To balance mussel size among treatments, mussels were binned according to length then randomly assigned from each bin to one of three groups: a group tested immediately ('field', $N=29$), an experimentally stressed group ('stressed', $N=83$) or a non-experimentally stressed group ('non-stressed', $N=83$). For 6.5 months (25 November 2019–12 June 2020), the stressed mussels were cyclically loaded (see 'Repeated loading treatment', below) approximately once a week for a total of 25 treatments in 29 weeks. Non-stressed mussels were removed from the tank weekly with the stressed mussels, replicating all components of the treatment except for the mechanical stress itself. We identified mussels throughout the experiment using small waterproof bee tags adhered with cyanoacrylate adhesive to the dorsal posterior quadrant of the right valve. At the end of 7 months, mussels were dissected, and their shell strength was measured (see 'Strength testing', below).

All mussels were housed together in a sheltered, outdoor aquarium system with sand-filtered, flow-through sea water (flow rate of $\sim 4 \text{ l min}^{-1}$). Mussels were housed in an $\sim 230 \text{ l}$ tank ($2.13 \text{ m} \times 0.53 \text{ m}$ footprint at 0.20 m water depth), and they were elevated off the base of the tank on a gravel-covered, plastic grate. For mussels in the intertidal zone, daily tidal rhythms affect many aspects of physiology (Andrade et al., 2018; Moyon et al., 2020) and, importantly, shell growth (Richardson, 1989). Because constant submersion can alter shell growth patterns (Richardson, 1989), the tank water level rose and fell in a twice daily high–low cycle to approximately mimic the natural tidal rhythms where the mussels were collected, shifting by 51 min daily. Mussels were fed 3 times a week at high tide by stopping water flow for at least 1 h and mixing into the tank 13 ml of marine microalgae concentrate diluted in ~ 1 liter of seawater (Shellfish Diet 1800, Instant Algae, Reed Mariculture, Campbell, CA, USA). After seawater flow was reinstated, the exchange of well-mixed tank water (4 l min^{-1} input to 230 l) was such that food concentration decreased by half approximately every 41 min (not accounting for food filtered by mussels).

Morphological measurements

We collected a suite of morphological measurements from all mussels in the study unless otherwise specified. Mussels were measured whole and live at the start of the experiment and before

dissection at the end of the experiment. We measured the mussel shell length, height and width with digital calipers (precision $\pm 0.01 \text{ mm}$); length was defined as the maximum distance along the anterior–posterior axis, height along the perpendicular dorsal–ventral axis, and width perpendicular to the aperture and including both valves as these measurements were taken from whole, live mussels (diagrams provided in Fig. S1 and all relevant data figures). We allowed mussels to gape, tipped them to spill the internal water, gently patted them dry, and weighed them ('wet mass'). If the mussel died during the course of the experiment, we were not always able to collect all final measurements.

At the end of the experiment, we dissected mussels by ventrally inserting a scalpel, severing the posterior adductor muscle, and gently prying the valves open. The internal soft tissue was gently removed by lightly scraping with a blunt nickel probe, and the gonads were separated. We patted both valves dry, then weighed each separately. We measured valve length, height and width as defined above for the whole shell, although each valve's width was measured separately. We also measured thickness at three locations: the apex of the dome (i.e. the point on the valve farthest from the aperture, and where width was measured), the midpoint of the hinge parallel to the aperture, and the dorsal lip just posterior of the hinge (diagrams provided in Fig. S1 and all relevant data figures). These thickness measurements were chosen because they could be consistently identified across individuals and represent different parts of the valve. Finally, we described the extent of internal repair. Mussels deposit distinct 'patches' on the internal surface, which are easily identified by their defined borders and matte texture (Crane et al., 2021). We categorized repair of each valve by approximating by eye the internal surface area covered by such patches: none, minimal ($<2 \text{ mm}^2$ patch surface area), low ($<25\%$ internal surface area patched), medium ($25\text{--}75\%$ internal surface area patched) or high ($>75\%$ internal surface area patched). Shells were immersed immediately in saltwater and strength tested the same day. Both soft tissue samples were dried at 60°C until the mass stabilized, and they were then weighed.

To provide detailed information about the prevalence of patching in the field, we collected additional mussels from the same site ($N=51$, length mean \pm s.d.: $37 \pm 5 \text{ mm}$; range: $29\text{--}51 \text{ mm}$) and from a second adjacent site higher in the intertidal zone ($1.6\text{--}2.0 \text{ m}$ above MLLW, $N=55$, length mean \pm s.d.: $35 \pm 4 \text{ mm}$; range: $25\text{--}44 \text{ mm}$). We did not exclude mussels based on external damage. Mussels were dissected within 3 days, and we measured only the live mussel wet mass and the valve mass, length, width and thickness at the apex of

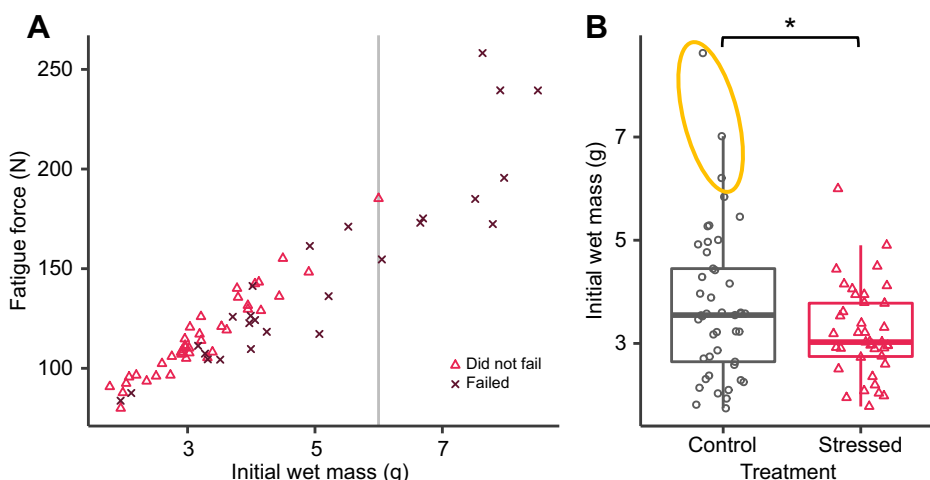


Fig. 1. Fatigue loading treatment introduced a size bias. (A) Among stressed mussels, the loading fatigue force scaled with size, such that a fraction of mussels of all sizes failed (crosses). However, all those that did not fail (triangles) were below a size threshold (gray line). (B) The resulting group of stressed mussels weighed less than control mussels (Welch two sample t -test: $t=2.0$, d.f.=73.2, $P<0.05$, mean difference 0.5 g). Boxes represent median and interquartile range (IQR); whiskers extend to the closest point not beyond $1.5 \times \text{IQR}$ outside the box with outliers falling beyond the whiskers; circles and triangles are individual data points. The orange ellipse indicates three control mussels larger than the largest surviving stressed mussel. $*P<0.05$.

the dome. We categorized internal repair as above, though further separating the medium category into two groups: medium low (25–50% internal surface area patched) and medium high (50–75% internal surface area patched). We also categorized the extent of external damage by binning based on surface area damaged (as above: none, minimal, low, medium low, medium high, high), and we used three different parameters to identify damage: full removal of the periostracum (i.e. exposing prismatic or deeper), full removal of the outer prismatic layer (i.e. exposing nacre or deeper) and full removal of the nacreous layer (i.e. exposing internal patches). For example, a single valve with medium low internal repair (25–50%) might be categorized as having high removal of the periostracum (>75%), medium low removal of the outer prismatic layer (25–50%), and minimal removal of the nacreous layer (<2 mm²). These damage metrics were not combined, but were instead each considered separately. Note that based on the initial filtering phase, all three groups of mussels in the primary experiment (stressed, non-stressed and field mussels) would be categorized as having none of the prismatic or nacreous layers fully removed.

Repeated loading treatment

Whole live mussels were repeatedly loaded with 15 compressive cycles to a predetermined force in a materials testing device. The force depended on mussel morphology, with scaling determined by a preliminary study of how mussel shell strength varied with wet mass [*post hoc* model of loading force: loading force (N)=46.1+[20.9×initial mussel wet mass (g)]; $F_{1,81}=580.1$, $R^2=0.88$, $P<0.001$; range: 80–258 N}. The force was applied perpendicular to the shell aperture by a flat plastic plate attached to a hydraulic ram and measured by a flat force plate on which the mussel rested; a series of scripts in MATLAB (version R2017b, MathWorks, Natick, MA, USA) controlled the hydraulic ram and synchronized data collection from the ram and force sensor (device and sensor described in Crane and Denny, 2020).

The hydraulic ram operated under displacement control; shells were loaded to the position at which the compressed force plate

provided the target force. Shells were loaded and then immediately unloaded with the ram moving at the same constant velocity in each direction, resulting in full loading–unloading cycle durations that ranged from 0.261 to 0.535 s across mussels. The mussel was oriented with the aperture parallel to the two plastic plates. The valve oriented downward was randomly determined for each mussel and consistent across all weeks. Mussels' orientation was maintained with a small piece of flexible modeling clay under the lower valve. Any mussels that experienced catastrophic failure of at least one valve during treatment were excluded from the remainder of the experiment.

For each mussel, we had 15 cycle–force maxima for every week of the experiment, and we used the following steps to calculate a single fatigue force value for each mussel. First, for every 15-cycle weekly stress treatment, we calculated the median of the force maxima for all 15 cycles that week ('weekly median force'). Second, we calculated the fatigue loading force for each mussel across the experiment as the mean of all the weekly median forces.

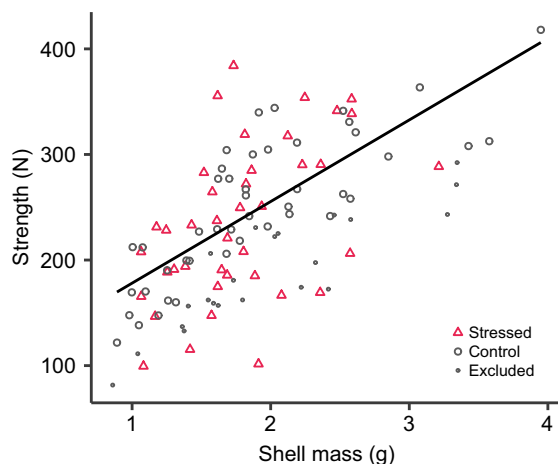


Fig. 2. The shells of chronically mechanically stressed mussels were not weaker than those of control mussels. To account for the 33.8% of stressed shells that broke during the repeated loading treatment, the weakest 33.8% of non-stressed shells, accounting for size, were excluded but are plotted here (small gray circles). The line shows multiple regression corresponding to ANCOVA with domedness held constant at the average [model: strength (N)=−221+77×shell mass (g)+894×domedness; ANCOVA results treatment: $F_1=0.46$, $P=0.50$, $SS=1154$; mass: $F_1=75.0$, $P<0.001$, $SS=188,912$; domedness: $F_1=11.8$, $P<0.001$, $SS=29,767$; residual d.f.=81, $SS=204,151$]. $N=40$ stressed, 45 control and 22 excluded non-stressed mussels.

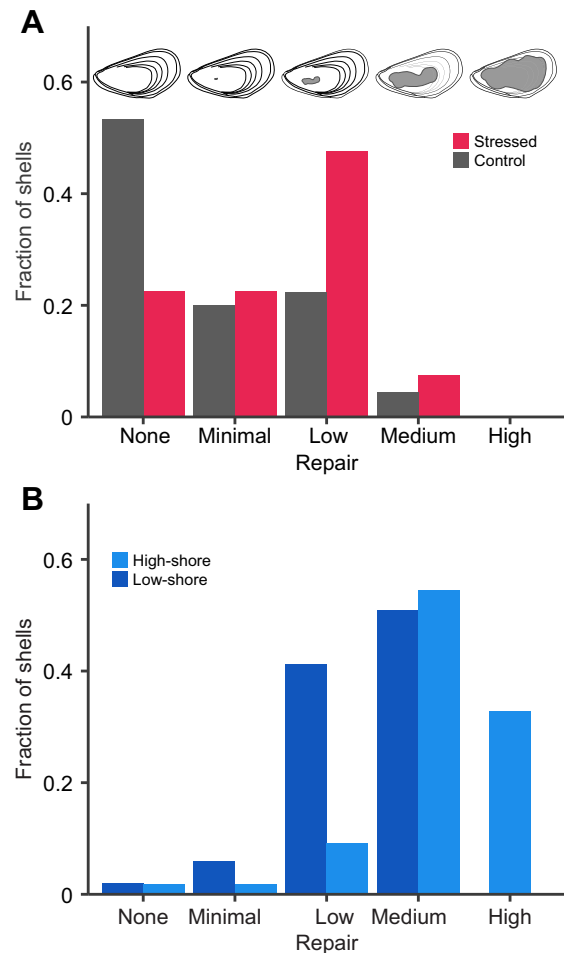


Fig. 3. Extent of internal patching for experimental and freshly collected mussels. (A) Stressed mussels tended to have more patching than control mussels (Wilcoxon rank sum test $W=582$, $P<0.01$, $N=85$ mussels: 40 stressed and 45 control). (B) Patching was common in mussels collected from the field, as indicated by the prevalence of internal patches of mussels collected from the same, low-shore site and from an adjacent high-shore site. Patching was more extensive in high-shore mussels (Wilcoxon rank sum test $W=672$, $P<0.001$, $N=106$ mussels: 51 low-shore and 55 high-shore). Hypothetical illustrations indicate the extent of patching appropriate for each category. Only data for the more extensively repaired valve of each shell are plotted.

This fatigue loading force was used for statistical analyses. The standard deviation for each mussel in cycle–force maxima across all the weeks (excluding the cycle during which the shell broke if this occurred), averaged 10 N or 8% of the average loading force (range: 0.8–31.5 N, 0.9–19.5%).

Strength testing

We tested the strength of the left and right valves independently for each mussel using the same materials testing device as for the repeated loading treatment. Valves were oriented with the aperture parallel to and resting on the force sensor. From each loading curve, we identified the breaking force as the force at catastrophic failure, and we refer to this force as the strength. Because we were interested in the strength of the mussel as a whole, we considered the weaker valve as representative of the shell's strength.

Statistical analyses

Accounting for mussel mortality

Between the first and second rounds of the repeated loading treatment, the broken shells of 18 of 161 mussels were found in the aquarium system, most likely attacked by a raccoon. The dead mussels were randomly distributed between stressed and non-stressed treatments (Pearson's Chi-squared test with Yate's continuity correction, $\chi^2=1.2$, d.f.=1, $P=0.27$), and they did not differ in length from the mussels that were not attacked (Welch two sample t -test, $t=-0.27$, d.f.=20.6, $P=0.79$). Excluding these mussels did not significantly alter the proportion of mussels that broke during the initial repeated loading treatment (change from 6.0% to 6.5%) and simplified all forthcoming analyses. We therefore

excluded these mussels from all analyses. No other similar events with fractured mussel shells occurred for the remainder of the experiment.

Additionally, during the 7 months of the experiment, 33.8% (26 of 77) of the stressed shells broke during the repeated loading treatment, reducing our stressed sample to only 51 mussels. We had based the target fatiguing force on how shell strength varied with wet mass (see above). However, while a fraction of mussels of all sizes broke, all the largest mussels broke (Fig. 1A). This resulted in the surviving stressed mussels being slightly smaller on average than control mussels (the 'control' group of non-stressed mussels defined in detail below) when considering wet mass (Fig. 1B, Welch two sample t -test: initial wet mass, $t=2.0$, d.f.=73.2, $P<0.05$, mean difference 0.52 g), though initial length did not differ (initial length, $t=1.7$, d.f.=80.3, $P=0.09$). Three control mussels were larger than the largest surviving stressed mussel, and repeating all subsequent analyses without these three control mussels did not significantly affect any of our conclusions.

Because we based the fatiguing force on how shell strength varied with size, we assumed the remaining mussels were approximately the 66.2% of mussels with the strongest shells for their size. This created a fundamental difference in the composition of the stressed and non-stressed groups of mussels. To allow comparison between these groups, we similarly filtered the non-stressed mussels to include only the 66.2% of mussels with the strongest shells; we fitted a multiple regression of non-stressed shell strength in terms of shell final length and domedness (the ratio of width to length), and we excluded the 33.8% of mussels with the most negative residuals. Henceforth, we refer to this reduced group as the 'control' mussels

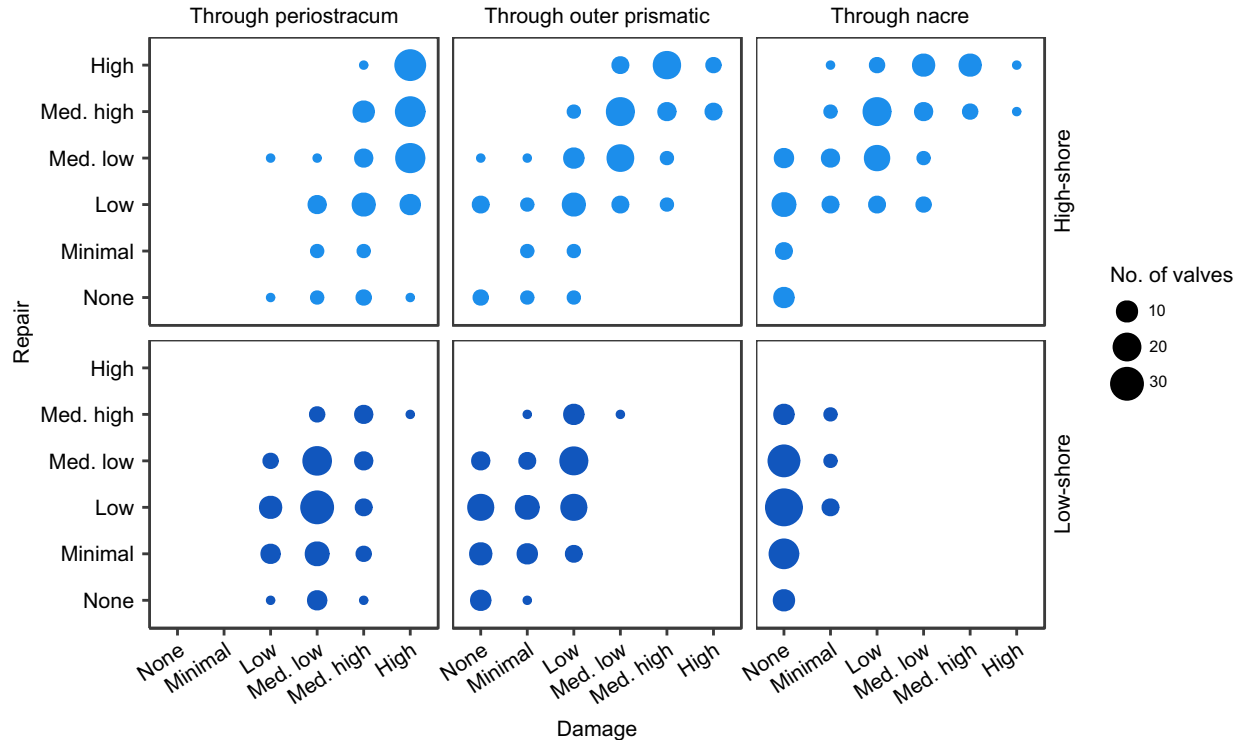


Fig. 4. External damage correlated with internal repair. Damage and repair were binned according to the surface area covered, and three different parameters were used to identify damage: removal of the periostracum, removal of the outer prismatic layer, and removal of the nacreous layer. Mussels from the low-shore site (bottom, $N=51$ mussels or 102 valves) were collected from the same location as those in the primary experiment, and a second group was collected higher in the intertidal zone (top, $N=55$ mussels or 110 valves). Spearman's rank order correlation for periostracum damage $S=75,988$, $\rho=0.62$, $P<0.001$; for prismatic damage $S=57,068$, $\rho=0.71$, $P<0.001$; for nacre damage $S=57,461$, $\rho=0.71$, $P<0.001$, $N=106$ mussels. Both valves of every mussel are included in the plot, though only one randomly selected valve of each mussel was included in analyses.

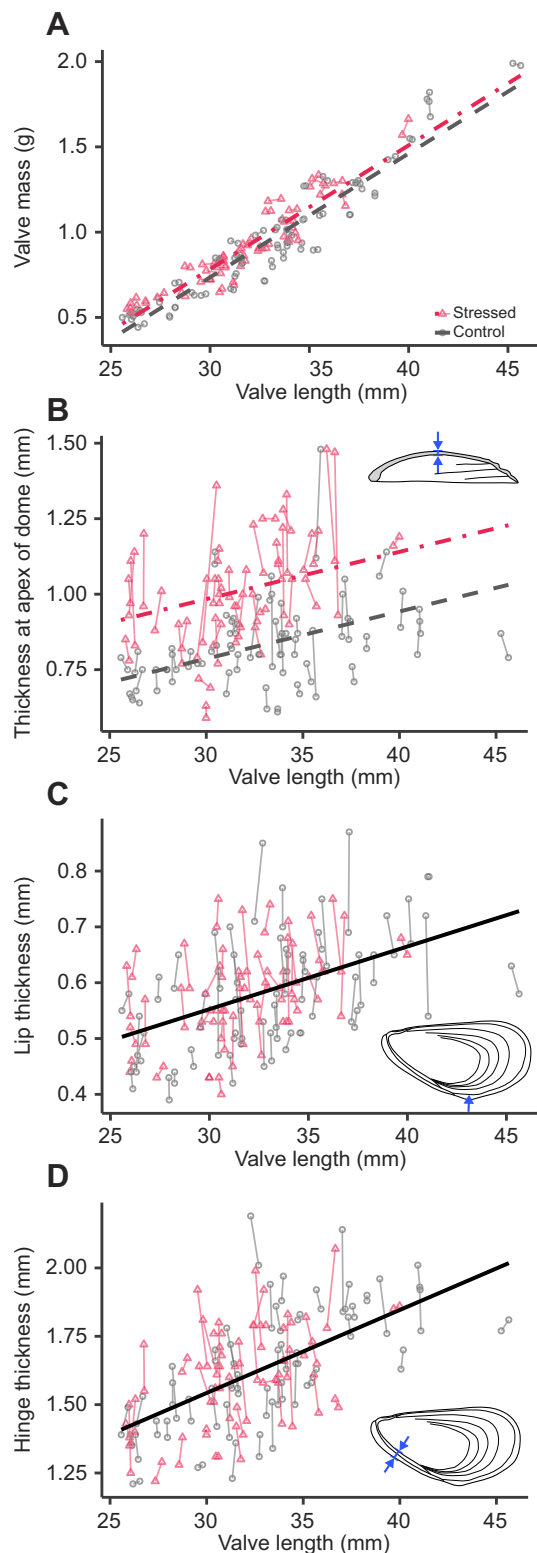


Fig. 5. In response to ongoing mechanical stress, mussel shells weighed more and thickened at the apex of the dome of the valve but not elsewhere. (A) Stressed mussel shells weighed more than control mussel shells (mixed effects model, Table 1). Colored lines between points connect valves of the same mussel. (B) Stressed mussel shells were also thicker at the apex of the dome than control mussel shells (Table 1). (C,D) Stressed mussel shells were not, however, thicker than control mussel shells at either the lip (C) or the hinge (D). Black lines show mixed effects models without treatment (Table 1). Schematic diagrams indicate thickness measurement locations: (B) shell in cross-section and bar between arrows indicates actual measurement, (C) arrow indicates where thickness was measured perpendicular to the plane of the diagram, and (D) bar between arrows indicates actual measurement.

intact shells, and the cause of death was not apparent. We report on and examine patterns associated with this mortality below (see ‘Does shell repair come at a cost?’, below). We excluded from subsequent analyses all mussels ($N=15$) found dead in such a manner that had not survived all 25 repeated loading treatments or, for non-stressed mussels, until the corresponding week.

All statistical analyses were conducted in R (version 3.3.2, <http://www.R-project.org/>).

Do mussels maintain shell repair in response to ongoing mechanical stress?

To test whether mussels were able to maintain repair in response to chronic mechanical stress, we compared the final strength of control and stressed shells using an analysis of covariance (ANCOVA) of strength in terms of treatment (stressed or control) with covariates of final shell mass and domedness, chosen because they have previously been shown to be significant predictors of strength and fatigue resistance for California mussel shells (Crane and Denny, 2020; Crane et al., 2021). We first confirmed normal distribution of the response variable in all treatment groups with a Shapiro–Wilk test (stressed mussels: $W=0.97$, $P=0.42$; control: $W=0.99$, $P=0.87$), and we confirmed homogeneity of slopes using multiple regression to test the significance of the interactions of each predictor variable ($P>0.05$).

In addition to looking at mussel strength, we compared internal evidence of physical repair between stressed and control mussels as well as between the low- and high-shore field mussels. We had categorized shell repair by binning the extent of repair patches across each valve’s internal surface. For each mussel, we considered only the valve with more extensive internal patching, and to match the experimental data, we collapsed the medium low and medium high bins for the low- and high-shore mussels. We then used a Wilcoxon rank sum test to compare the distribution of shells within the bins between the stressed and control mussels. We repeated this analysis between the low- and high-shore mussels.

We also used the low- and high-shore mussels from the field to assess the relationship between the extent of external damage and the extent of internal repair. We randomly selected one valve from each mussel then calculated the Spearman’s rank correlation between damage and repair separately for each type of damage.

Does mechanical stress trigger morphological changes?

We tested whether stressed mussels had thickened relative to control mussels by comparing valve mass and thickness between stressed and control mussels with a linear mixed effects model of final valve mass or thickness in terms of treatment and valve length with a random effect of individual (fitted in R, nlme, version 3.1.137; <https://CRAN.R-project.org/package=nlme>). We fitted these models separately for the three measures of thickness: thickness at

($N=46$, distinct from the non-stressed mussels, which includes the full group: $N=71$).

Finally, 23 weeks after the experiment started and on most subsequent weeks, we found a few mussels dead in the aquarium system, resulting in 23 dead mussels total. Unlike the fractured mussels found during the second week, these mussels had fully

the apex of the dome, thickness at the hinge, and thickness at the dorsal lip just posterior of the hinge. We reduced models by removing non-significant predictors.

We also looked at gross morphological differences. Because we measured mussel size at both the beginning and end of the 7 month experiment, we were able to directly compare growth between stressed and control mussels. By subtracting initial from final measurements of length, height, width and mussel wet mass, we quantified growth across each of these dimensions. We also looked at relative changes by comparing the changes in the aperture roundness (the ratio of shell height to length) and the shell domedness (width to length). For each metric, we first conducted a one-sample *t*-test to assess whether the average growth in each group (stressed and control) differed from zero. We then conducted a Welch two sample *t*-test comparing growth of the stressed and control mussels for each metric. Note that no analyses of wet mass included any mussels that had died of unknown causes, even if they survived to the final week, as wet mass was not measured for mussels that were already dead.

Finally, we assessed morphological changes taking shell orientation during repeated loading treatment into account. Which valve was oriented up or down was randomly determined at the start of the study and was consistent across all weeks. Among shells that broke during repeated mechanical loading, we counted the frequency of the top and/or bottom valves breaking. In cases where both valves broke, we were not able to determine which valve broke first, so both valves were counted as having broken. Among the stressed mussels at the end of the experiment, we then assessed whether there were morphological differences between the valve on top during loading and the valve on the bottom. We used paired *t*-tests to compare the length of the top and bottom valves, and we repeated this analysis for valve height, valve width, valve mass, and thickness at the apex of the dome, the lip and the hinge.

Does shell repair come at a cost?

We tested whether maintaining shell repair in response to repeated mechanical stress came at a cost to mussel health or reproduction. First, we considered the amount of living soft tissue contained within the shell. For both gonad and non-gonad tissue, we compared the dry tissue mass between stressed and control mussels as well as the initial group of mussels dissected and tested immediately after collection ('field' group). We constructed multiple regression models of the log-transformed dried mass of the internal

non-gonad tissue in terms of the log-transformed shell mass, the treatment and an interaction term. We constructed models separately for each comparison (stressed versus control, stressed versus field, field versus control), and we removed any non-significant interaction terms from the models. We repeated these analyses with the log-transformed dried mass of the gonad tissue. We also calculated relative investment in reproductive capacity using the ratio of the dry gonad mass to the dry mass of all the internal tissue. This ratio was not normally distributed in all groups (Shapiro–Wilk test $P < 0.05$), so we compared the ratio between groups with a Kruskal–Wallis test followed by pairwise comparisons with Wilcoxon rank sum tests and a Bonferroni correction. Note that tissue mass was not measured or analyzed for any mussels that had died of unknown causes, even if they survived to the final week.

Additionally, we compared mortality as a metric of health between the stressed and non-stressed mussels. We evaluated the group of mussels that died of unknown causes starting 23 weeks after the experiment began. We used Chi-squared analyses to compare the number of mussels found dead in this manner against those that survived between stressed and non-stressed mussels.

RESULTS

Do mussels maintain shell repair in response to ongoing mechanical stress?

After 7 months of weekly mechanical stress, the shells of stressed mussels were not weaker than those of control mussels (Fig. 2; ANCOVA $F_{1,81}=0.46$, $P=0.50$, $SS=1154$, residual $SS=204,151$); both covariates in the ANCOVA – shell mass ($F_{1,81}=75.0$, $P<0.001$, $SS=188,912$) and domedness ($F_{1,81}=11.8$, $P<0.001$, $SS=29,767$) – were correlated with strength.

Stressed mussels also had significantly more internal patching than control mussels (Fig. 3A; Wilcoxon rank sum test $W=582$, $P<0.01$, $N=85$ mussels). Patches were found extensively in field-collected mussels, though low-shore mussels had less patching than high-shore mussels (Fig. 3B; Wilcoxon rank sum test $W=672$, $P<0.001$, $N=106$ mussels).

Internal patching was correlated with each of the three metrics of external damage (Fig. 4; Spearman's rank order correlation for periostracum damage $S=75,988$, $\rho=0.62$, $P<0.001$; for prismatic damage $S=57,068$, $\rho=0.71$, $P<0.001$; for nacre damage $S=57,461$, $\rho=0.71$, $P<0.001$, $N=106$ mussels).

Table 1. Linear mixed effects models of valve mass and thickness at different locations in terms of valve length and treatment (control or stressed), with a random effect of individual

Metric	N (valves, mussels)	Model	AIC	Coefficient	Value	s.e.	<i>t</i>	<i>P</i> -value
Valve mass	170,85	Full	−477	Intercept	−1.44	0.09	−16.2	<0.001
				Length	0.07	0.00	27.3	<0.001
				Stressed	0.05	0.02	2.2	<0.05
Dome apex thickness	170,85	Full	−164	Intercept	0.32	0.12	2.7	<0.01
				Length	0.02	0.00	4.5	<0.001
				Stressed	0.20	0.03	7.1	<0.001
Lip thickness	170,85	Full	−364	Intercept	0.20	0.07	2.9	<0.01
				Length	0.01	0.00	5.7	<0.001
				Stressed	0.02	0.02	0.9	0.35
		Reduced	−371	Intercept	0.22	0.07	3.3	<0.01
				Length	0.01	0.00	5.6	<0.001
				Stressed	0.01	0.03	0.4	0.68
Hinge thickness	170,85	Full	−154	Intercept	0.62	0.14	4.4	<0.001
				Length	0.03	0.00	7.4	<0.001
				Stressed	0.01	0.03	0.4	0.68
		Reduced	−160	Intercept	0.63	0.13	4.7	<0.001
				Length	0.03	0.00	7.4	<0.001
				Stressed	0.01	0.03	0.4	0.68

Does mechanical stress trigger morphological changes?

A linear mixed effects model with mussel as a random effect showed that stressed mussels were, on average, 0.05 ± 0.02 g or 5% heavier and 0.20 ± 0.03 mm or over 20% thicker at the apex of the dome than control mussels (Fig. 5A,B, Table 1). However, stressed mussels did not differ from controls in their thickness at either the hinge or dorsal lip (Fig. 5C,D, Table 1).

Between the start and end of the experiment, stressed and control mussels both grew slightly but significantly along all measured dimensions (Fig. 6). One-sample *t*-tests indicated they increased in wet mass (control: $t=8.38$, d.f.=41, $P<0.001$, mean growth 0.35 g; stressed: $t=8.71$, d.f.=35, $P<0.001$, mean growth 0.37 g), length (control: $t=2.36$, d.f.=44, $P<0.05$, mean growth 0.11 mm; stressed: $t=2.94$, d.f.=39, $P<0.01$, mean growth 0.08 mm), height (control: $t=3.80$, d.f.=44, $P<0.001$, mean growth 0.07 mm; stressed: $t=5.44$, d.f.=39, $P<0.001$, mean growth 0.09 mm) and width (control: $t=10.48$, d.f.=44, $P<0.001$, mean growth 0.17 mm; stressed: $t=7.52$, d.f.=39, $P<0.001$, mean growth 0.10 mm). Mussel shells of both groups also became more domed (control: $t=6.47$, d.f.=44, $P<0.001$; stressed: $t=4.64$, d.f.=39, $P<0.001$). However, control mussels did not change in aperture roundness ($t=0.66$, d.f.=44,

$P=0.51$), though stressed mussels had a marginal increase in aperture roundness ($t=2.02$, d.f.=39, $P=0.05$).

Comparing growth between stressed and control mussels, they did not differ significantly in their growth in most morphological measurements (Fig. 6), including wet mass (Welch two sample *t*-test $t=-0.26$, d.f.=75.5, $P=0.80$), length ($t=0.53$, d.f.=70.46, $P=0.60$) and height ($t=-0.57$, d.f.=81.85, $P=0.57$), and the associated roundness of the aperture (height:length, $t=-0.95$, d.f.=82.81, $P=0.35$). However, control shell width did, on average, increase by 0.07 mm more than that of stressed shells, a 65% greater increase ($t=3.16$, d.f.=82.02, $P<0.01$). This increase in width corresponded to control shells increasing more in domedness (width:length, $t=2.19$, d.f.=80.67, $P<0.05$).

Considering mussel shell orientation during repeated loading treatments, among the mussels whose shells failed, the top valve almost always failed (23/25 mussels) and the bottom valve failed just under half the time (12/25 mussels; Fig. 7A). Furthermore, at the end of the 7 month study, some differences emerged in the morphology of the top and bottom valves (Fig. 7). Valves that had been on top during loading did not differ in their final length or width from valves on the bottom (paired *t*-test length: $t=-0.38$,

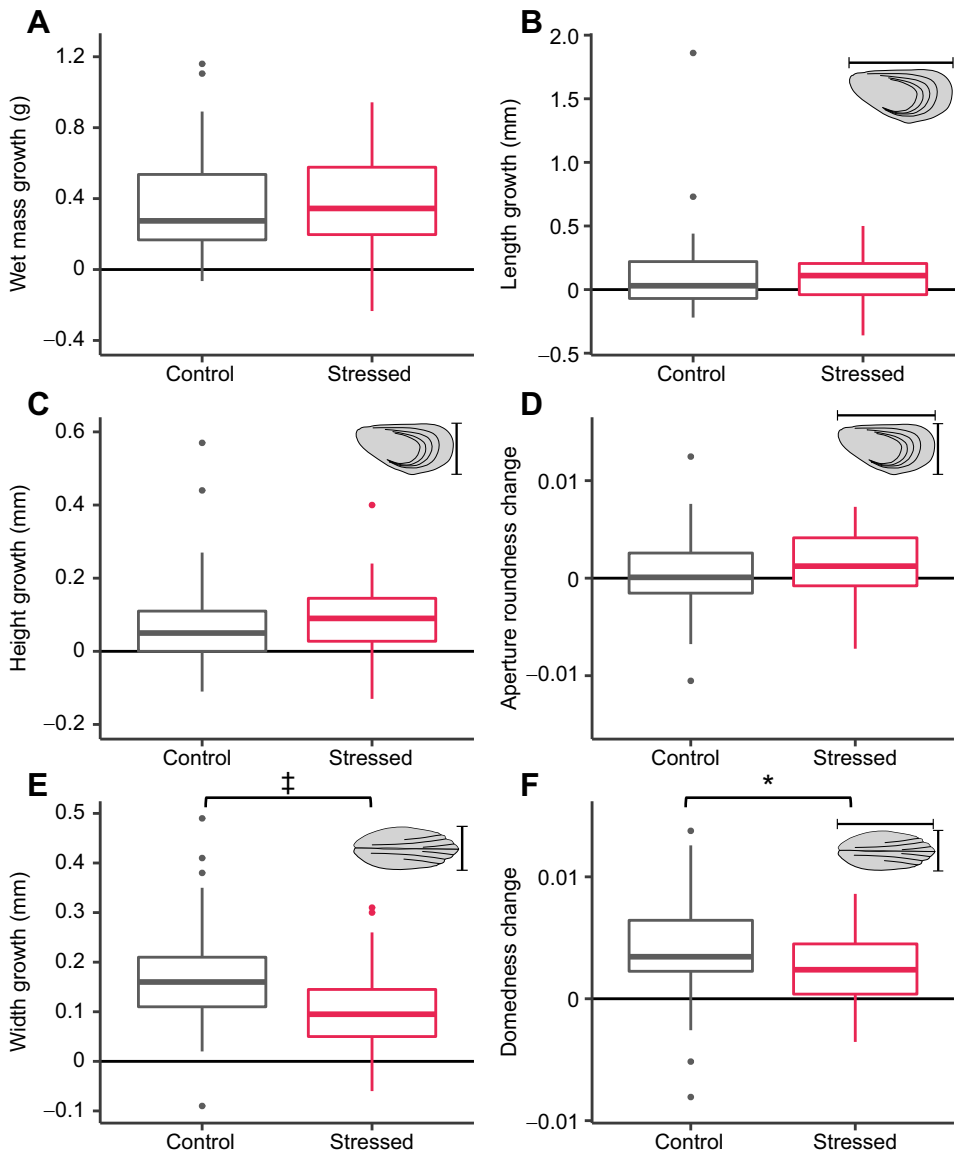


Fig. 6. Stressed and control mussels grew between the start and end of the 7 month experiment. (A,B) Stressed and control mussels did not differ in how much they increased in wet mass (A) and length (B) (wet mass: $t=-0.26$, d.f.=75.5, $P=0.80$; length: $t=0.53$, d.f.=70.46, $P=0.60$). (C,D) They also did not differ in their change in height (C) or the roundness of the aperture (D) (height:length ratio; height: $t=-0.57$, d.f.=81.85, $P=0.57$; aperture roundness: $t=-0.95$, d.f.=82.81, $P=0.35$). (E,F) However, control mussels increased in width (E) by 65% more than stressed mussels ($t=3.16$, d.f.=82.02, $P<0.01$), resulting in a greater increase in domedness (F) (width:length; $t=2.19$, d.f.=80.67, $P<0.05$). Schematic diagrams illustrate the relevant measurements. (A) $N=42$ control and 36 stressed mussels, (B–F) $N=45$ control and 40 stressed mussels. * $P<0.05$, † $P<0.01$. Boxes represent median and IQR; whiskers extend to the closest point not beyond $1.5 \times \text{IQR}$ outside the box with outliers falling beyond the whiskers.

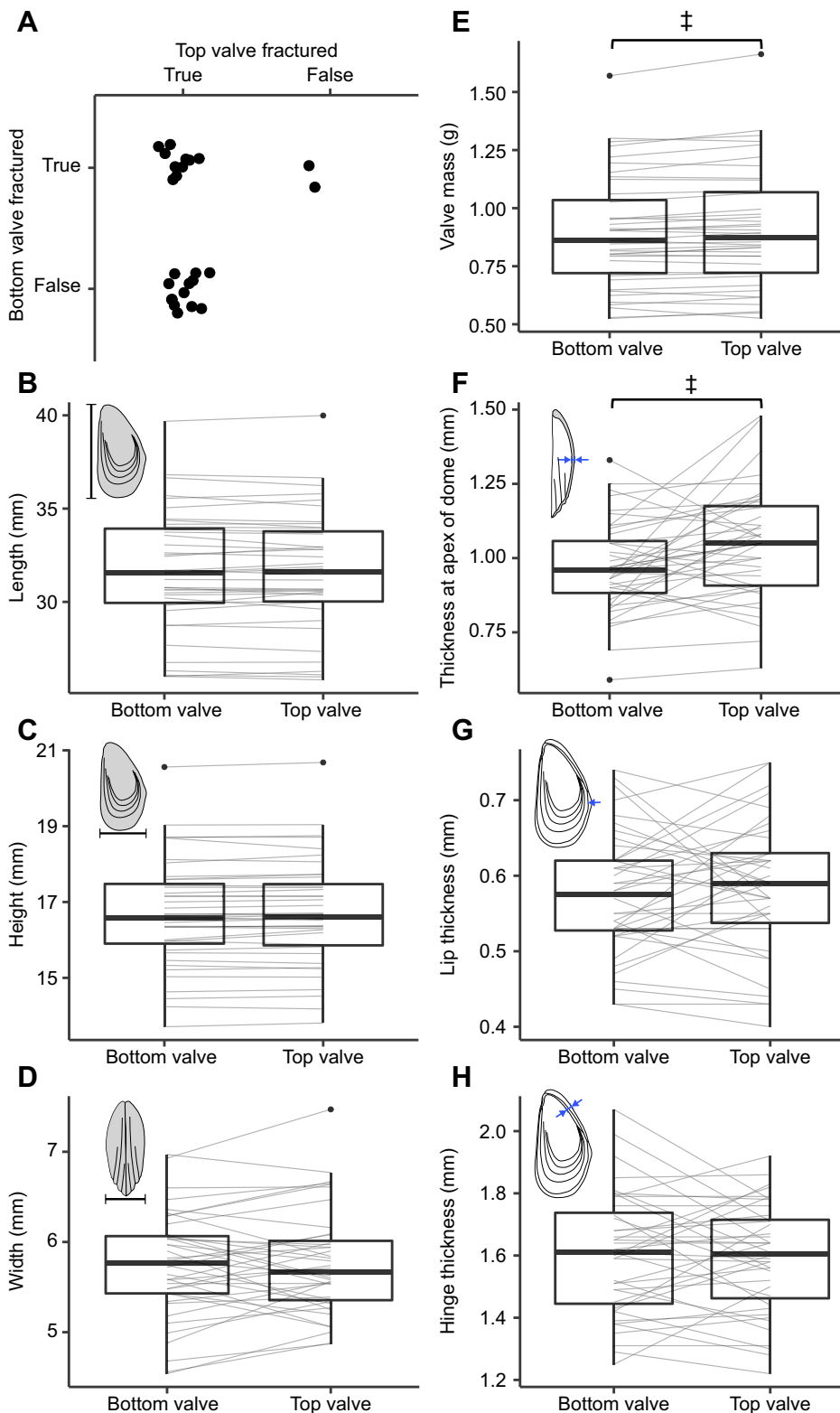


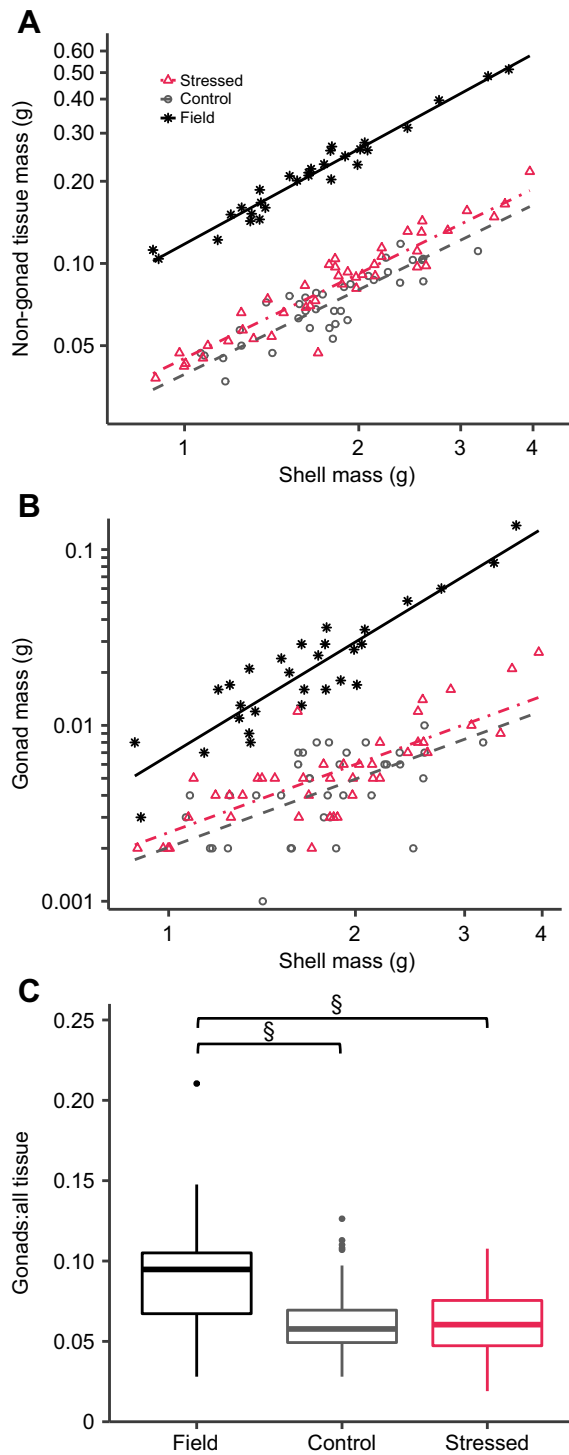
Fig. 7. Shell orientation during repeated loading treatment affected breakage and repair. Orientation was random and consistent throughout the study. (A) The top valve usually broke, whereas the bottom valve sometimes broke and sometimes did not. (B–D) At the end of the study, valves that had been on top did not differ in their length (B) or width (D) from valves on the bottom, though height (C) was close to obtaining marginal significance (paired *t*-test length: $t=-0.38$, d.f.=39, $P=0.71$; height: $t=1.95$, d.f.=39, $P=0.06$; width $t=0.48$, d.f.=39, $P=0.63$). (E) Valves on top during loading on average weighed 0.014 g more than their counterparts ($t=3.25$, d.f.=39, $P<0.01$). (F–H) Top valves also tended to be thicker at the apex of the dome (F; $t=2.94$, d.f.=39, $P<0.01$), with no difference in thickness at the lip (G; $t=0.67$, d.f.=39, $P=0.51$) or at the hinge (H; $t=-0.49$, d.f.=39, $P=0.63$). $^{\dagger}P<0.01$. Boxes represent median and IQR; whiskers extend to the closest point not beyond $1.5\times\text{IQR}$ outside the box with outliers falling beyond the whiskers. Light gray lines connect valves from the same mussel. Schematic diagrams indicate measurement locations: (B–D) measurement was the longest dimension defined by the black bar; (F,H) blue bar between arrows indicates actual measurement, and (G) blue arrow indicates where thickness was measured perpendicular to the plane of the diagram.

d.f.=39, $P=0.71$; width $t=0.48$, d.f.=39, $P=0.63$), but, with marginal significance, top valves had on average 0.03 mm more height ($t=1.95$, d.f.=39, $P=0.06$). Valves on top during loading also weighed on average 0.014 g more than their counterparts on the bottom ($t=3.25$, d.f.=39, $P<0.01$). Considering valve thickness, top valves tended to be 0.08 mm thicker at the apex of the dome ($t=2.94$, d.f.=39, $P<0.01$), with no difference in thickness at the lip

($t=0.67$, d.f.=39, $P=0.51$) or at the hinge ($t=-0.49$, d.f.=39, $P=0.63$).

Does shell repair come at a cost?

Mussels lost non-shell body mass during the 7 months they were maintained in the laboratory. Mussels dissected immediately after collection from the field had relatively more soft tissue and gonad



mass than either stressed or control mussels, and there was an interaction between size and treatment such that the difference was even greater for larger mussels (Fig. 8A,B, Table 2). Furthermore, stressed mussels had even less tissue mass than control mussels; compared with control mussels they had, on average ~87% as much soft tissue and ~82% as much gonad mass (Fig. 8A,B, Table 2). It is important to note that the difference in gonad mass between stressed and control mussels lost significance ($P>0.05$) when the three largest control mussels were excluded from analyses as discussed above (see ‘Accounting for mussel mortality’).

Fig. 8. Mussels lost tissue mass while stored in the laboratory, and more so if chronically stressed. (A) Stressed mussels had ~87% the non-gonad soft tissue of control mussels, and both groups stored in the lab had much less soft tissue than mussels from the field, especially in the case of larger mussels (models reported in Table 2: regression for stressed and control mussels taken from the stressed versus control model, and field mussel regression taken from stressed versus field model). (B) The same pattern was found when considering only the gonads (models reported in Table 2: regression for stressed and control mussels taken from the stressed versus control model, and field mussel regression taken from stressed versus field model). (C) Field-collected mussels had significantly more gonads for their total internal tissue mass than either control or stressed mussels, which did not differ from each other (Kruskal–Wallis $\chi^2=17.7$, d.f.=2, $P<0.001$). $N=29$ field, 42 control and 36 stressed mussels. § $P<0.001$. Boxes represent median and IQR; whiskers extend to the closest point not beyond $1.5\times\text{IQR}$ outside the box with outliers falling beyond the whiskers.

The ratio of dry gonad mass to dry mass of all the internal tissue differed significantly between treatment groups (Fig. 8C; Kruskal–Wallis $\chi^2=17.7$, d.f.=2, $P<0.001$). *Post hoc* Wilcoxon rank sum tests revealed that the field mussels had significantly higher ratios (relatively more gonads) than either the control ($P<0.001$, difference=0.029) or stressed ($P<0.001$, difference=0.031) mussels, which did not differ from each other ($P=1.00$).

When considering mortality in the final weeks of the experiment, stressed mussels were more likely to die of unknown causes (29% died, 15/51 mussels) than non-stressed mussels, of which only 11% died (8/71 mussels; Pearson’s Chi-squared=5.26, d.f.=1, $P<0.05$).

DISCUSSION

Mussels were able to maintain repair of their shell after 7 months of experiencing significant weekly mechanical stress. Although mussel shells are weakened by repeated loading (Crane and Denny, 2020; Crane et al., 2021), after 7 months of repeated force application, stressed shells were just as strong as those of non-stressed control mussels (Fig. 2), and they had more patches across their internal surface (Fig. 3A, Table 1). These patches were also found extensively on mussel shells in the field, and their presence was correlated with the extent of external shell damage (Figs 3B and 4). Stressed mussels also showed small though significant morphological changes. In addition to weighing more and thickening at the apex of the dome, stressed mussels increased 39% less in width across the seven months than did control mussels, resulting in less increase in domedness (Figs 5 and 6). All of the mussels fared poorly in the laboratory setting, but maintaining ongoing shell repair did come at an elevated cost, with even greater tissue loss and greater mortality for stressed mussels than control mussels (Fig. 8, Table 2).

These findings demonstrate that mussels can continue to repair their shells in response to chronic mechanical stress. Throughout its life, a California mussel faces repeated mechanical insults from predators and the environment. Many of these, though not lethal individually, cause damage that weakens a shell and makes it more susceptible to breakage in the future (Crane and Denny, 2020). Given this accumulating threat, mussels need to be able to mount a rapid repair response that can be maintained against repeated encounters. The fatiguing forces used in this experiment ranged from 80 to 260 N, which encompasses the crushing forces of a variety of crabs from the Pacific Northwest of the USA (Taylor, 2000) and which could be representative of other predators as well as of environmental threats, such as impacts from wave-hurled debris (Shanks and Wright, 1986). The capacity to maintain shell repair for an extended duration may be an important component of

Table 2. Multiple regression models of dried tissue mass (of either non-gonad or gonad tissue) in terms of shell mass, treatment and an interaction term

Comparison	y	F	d.f.	N	P-value	R ²	Coefficient	Value	s.e.
Control vs field	log ₁₀ (tissue mass)	962	2,68	71	<0.001	0.97	intercept	−0.92 [§]	0.01
							log ₁₀ (shell mass)	1.10 [§]	0.04
							control	−0.45 [§]	0.01
Stressed vs field	log ₁₀ (tissue mass)	584	3,61	65	<0.001	0.97	intercept	−0.93 [§]	0.02
							log ₁₀ (shell mass)	1.16 [§]	0.07
							stressed	−0.45 [§]	0.03
							interaction	−0.22*	0.10
Stressed vs control	log ₁₀ (tissue mass)	232	2,75	78	<0.001	0.86	intercept	−1.35 [§]	0.02
							log ₁₀ (shell mass)	1.03 [§]	0.05
							stressed	−0.06 [§]	0.01
Control vs field	log ₁₀ (gonad mass)	141	3,67	71	<0.001	0.86	intercept	−2.17 [§]	0.05
							log ₁₀ (shell mass)	2.14 [§]	0.21
							control	−0.46 [§]	0.07
Stressed vs field	log ₁₀ (gonad mass)	103	3,61	65	<0.001	0.84	interaction	−0.76 [‡]	0.26
							intercept	−2.17 [§]	0.06
							log ₁₀ (shell mass)	2.14 [§]	0.24
							stressed	−0.47 [§]	0.10
Stressed vs control	log ₁₀ (gonad mass)	40.2	2,75	78	<0.001	0.52	interaction	−1.07 [‡]	0.36
							intercept	−2.61 [§]	0.05
							log ₁₀ (shell mass)	1.29 [§]	0.15
							stressed	−0.08*	0.04

Mass measurements were in grams. Significance of coefficients is indicated as: * $P < 0.05$, $^{\dagger}P < 0.01$, $^{\S}P < 0.001$. Separate models compared control versus stressed mussels (with control as the baseline), field versus stressed mussels (with field as the baseline), and control versus field mussels (with field mussels as the baseline).

the California mussel's success in the harsh environment of the wave-swept rocky coast.

Physical repair and morphological changes

The long-term nature of this experiment allowed us to identify physical patterns of repair, specifically patching and thickening. Stressed shells had increased patching across their internal surface, where shell is deposited. Similar patches have been described in response to other kinds of external wear in other mollusks (Cadée, 1999; O'Neill et al., 2018; Peck et al., 2018), and here we demonstrate that they are correlated with external damage, and document them in response to ongoing compressive mechanical stress. Additionally, stressed shells weighed more and were thicker than control shells at the apex of the dome, though not at measured locations on the hinge and lip. This evidence of repair converges with research about where mussel shells break: whole mussels under cyclic compression in this orientation more often show fractures at or near the apex of the dome, where we documented thickening, as compared with more distally around the aperture (Crane et al., 2021). We did not record the location of patches relative to thickening, so we cannot determine the extent to which patching contributed to thickening at the apex of the dome, though it seems likely these two findings are related. Both the patching and thickening indicate a targeted shell repair response, and more extensive measurements of shell thickness, patch location and morphology, and damage accumulation could indicate the exact amount of localization.

Further evidence of a targeted thickening response can be found when considering mussel orientation during loading. Patterns of failure offer circumstantial evidence that the top valve during weekly loading experienced greater stress concentration; among mussels that failed, the top valve almost always failed (23/25 mussels) whereas the bottom valve failed only about half the time (12/25 mussels; Fig. 7A). Given valve orientation was randomly assigned, we do not think it likely this is due to consistent mechanical or morphological differences between top and bottom

valves at the start of the study. Instead, we suspect that the small pieces of modeling clay placed under the bottom valve to stabilize the mussel also distributed stresses more evenly across the bottom valve. Additionally, at the end of the study, among stressed mussels that did not fail, top valves were heavier and thicker at the apex of the dome than their counterpart bottom valves (Fig. 7E,F). We did not directly compare stresses across locations within each valve, so we cannot definitively attribute these morphological differences to greater stress concentrations on the top valve; however, taken together, the failure rates and morphological differences suggest mussels are specifically targeting a response of thickening and increasing mass to valves at greater risk.

In addition to internal thickening, repeated mechanical loading triggered small but significant differences in growth across the 7 months of the experiment. On average, mussels grew slightly in all measured dimensions during the experiment, but shell width and the associated relative metric, domedness, increased less for stressed mussels than for control mussels. Thickening is an intuitive correlate to patching, and it is often associated with strength (Boulding, 1984; Crofts and Summers, 2014) and documented in studies of shell plasticity in response to the presence of predators or environmental threats (Bourdeau, 2010; Bourdeau and Padilla, 2019; Harper et al., 2012; Leonard et al., 1999; Palmer, 1990). By contrast, it is initially surprising that repeatedly stressed shells increased less in width and domedness. Were mussels changing shell form to be more fracture and fatigue resistant, we would instead have expected stressed shells to ultimately be wider and more domed, morphological features associated with strength and fatigue resistance in California mussel shells (Crane and Denny, 2020). One potential explanation for this result is that mechanically stressed mussels were investing limited resources in building a thicker shell as opposed to investing in widening the shell, and that, ultimately, this thickening allowed mussels to maintain strength despite a flatter shell. These small differences highlight the importance of long-term tracking to identify morphological changes; in future work, further insight might be gained with

an even longer-running experiment or with younger mussels, whose shell form may be more plastic.

Cost of ongoing shell repair and conclusions

Two lines of evidence suggest that maintaining shell repair in response to ongoing mechanical stress comes at a cost to mussels: mortality and loss of tissue mass. These negative effects are significant, though they are relatively small compared with the high cost to mussels of being maintained in the laboratory for 7 months – an experimental necessity to control exposure to mechanical stress. All mussels in the experiment, mechanically stressed or not, experienced substantial loss of tissue and gonad mass, especially larger mussels, as well as increased mortality in the final weeks of the experiment. We suspect these effects were primarily due to insufficient food. Although constant submersion would have increased feeding time, we prioritized mimicking the tidal fluctuations these intertidal mussels would naturally experience in the field. Significantly for our conclusions, though, stressed mussels fared still worse than control mussels. Stressed mussels lost more tissue and gonad mass and were more likely to die from unknown causes. These results demonstrate a clear and significant loss of fitness for mussels experiencing ongoing mechanical stress.

Our experiment allowed us to quantify the cost of maintaining repair for mussels stored in the laboratory, but of course, the question of interest is the cost to mussels in the field. We know that both experimental stress treatment and lab storage were detrimental to tissue mass and survival (Fig. 8). The cost of maintaining repair may be consistent in the lab and the field, such that the cost of maintaining repair for stressed mussels in the field can be extrapolated from our data. However, the cost of being in the lab and the cost of repair may instead interact. Food limitation could exacerbate the cost of ongoing repair, which may be minor under ideal environmental conditions. Alternatively, the effects of food limitation may have masked the cost of ongoing repair, such that fatigue under ideal conditions is more costly than it appears in our study, particularly with respect to reproductive capacity. We cannot distinguish these alternatives using our data, but they are worth considering. The potentially shifting cost of repair under different environmental conditions is important for transferring our conclusions to the field, and is vital in the context of climate change. The effects of climate change on shell structure, shell mechanics and the cost of shell deposition are all well studied (Fitzer et al., 2015; Gaylord et al., 2011; Melzner et al., 2011), and the cost of ongoing shell maintenance may be another component to how climate change affects hard-shelled mollusks.

In response to ongoing mechanical stress, many biological systems can repair damaged structures and mount broader plastic changes. Bone has a well-documented capacity to resorb and remodel depending on mechanical stimuli (Arola et al., 2010; Burr, 2002; Currey, 2002); many plants similarly will change growth rate and mechanical properties (Goodman and Ennos, 1996; Jaffe, 1973; Jaffe et al., 1984; Stokes et al., 1995). Our research has extended these perspectives to an external armor system – and within research on external armor, expanded research to include the capacity to respond to ongoing mechanical stimuli. Mussels, even at a cost to their health, can thicken and change shell form to maintain strength. Incorporating the interplay between the accumulation of damage from repeated encounters and the cost of repair in response to this damage provides a nuanced and ecologically significant lens through which to understand hard external armor.

Acknowledgements

We would like to thank Tom Rolander, Tom Hata, John Lee and Chris Garsha for assistance in designing and building experimental equipment. We would like to thank Atish Agarwala and Benjamin Burford for discussions of statistics and interpretation of results. We thank Jonathan Payne, Jeremy Goldbogen, Christopher Lowe, Benjamin Burford and Nicole Moyer for feedback throughout. Nicole Moyer assisted with animal care and feeding. We also thank two anonymous reviewers for feedback on the manuscript.

Competing interests

The authors declare no competing or financial interests.

Author contributions

Conceptualization: R.L.C., M.W.D.; Methodology: R.L.C., M.W.D.; Software: R.L.C.; Formal analysis: R.L.C.; Investigation: R.L.C.; Resources: R.L.C., M.W.D.; Data curation: R.L.C.; Writing - original draft: R.L.C.; Writing - review & editing: R.L.C., M.W.D.; Visualization: R.L.C.; Funding acquisition: R.L.C., M.W.D.

Funding

This work was supported by the National Science Foundation (grant IOS-1655529 to M.W.D.), the National Science Foundation Graduate Research Fellowship program (grant DGE-1147470 to R.L.C.), and the Dr Earl H. Myers and Ethel M. Myers Oceanographic and Marine Biology Trust (grant to R.L.C.).

Data availability

Data and code are available from Mendeley: doi:10.17632/fm239hdxh9.1

References

- Andrade, M., Soares, A., Figueira, E. and Freitas, R. (2018). Biochemical changes in mussels submitted to different time periods of air exposure. *Environ. Sci. Pollut. Res.* **25**, 8903–8913. doi:10.1007/s11356-017-1123-7
- Arola, D., Bajaj, D., Ivancik, J., Majd, H. and Zhang, D. (2010). Fatigue of biomaterials: hard tissues. *Int. J. Fatigue* **32**, 1400–1412. doi:10.1016/j.ijfatigue.2009.08.007
- Blundon, J. A. and Vermeij, G. J. (1983). Effect of shell repair on shell strength in the gastropod *Littorina irrorata*. *Mar. Biol.* **76**, 41–45. doi:10.1007/BF00393053
- Boulding, E. G. (1984). Crab-resistant features of shells of burrowing bivalves: decreasing vulnerability by increasing handling time. *J. Exp. Mar. Biol. Ecol.* **76**, 201–223. doi:10.1016/0022-0981(84)90189-8
- Boulding, E. G. and LaBarbera, M. (1986). Fatigue damage: repeated loading enables crabs to open larger bivalves. *Biol. Bull.* **171**, 538–547. doi:10.2307/1541622
- Bourdeau, P. E. (2010). An inducible morphological defence is a passive by-product of behaviour in a marine snail. *Proc. R. Soc. B Biol. Sci.* **277**, 455–462. doi:10.1098/rspb.2009.1295
- Bourdeau, P. E. and Padilla, D. K. (2019). Cue specificity of predator-induced phenotype in a marine snail: is a crab just a crab? *Mar. Biol.* **166**, 84. doi:10.1007/s00227-019-3526-0
- Burr, D. B. (2002). Targeted and nontargeted remodeling. *Bone* **30**, 2–4. doi:10.1016/S8756-3282(01)00619-6
- Cadée, G. C. (1999). Shell damage and shell repair in the Antarctic limpet *Nacella concinna* from King George Island. *J. Sea Res.* **41**, 149–161. doi:10.1016/S1385-1101(98)00042-2
- Chen, Y., Liu, C., Li, S., Liu, Z., Xie, L. and Zhang, R. (2019). Repaired shells of the pearl oyster largely recapitulate normal prismatic layer growth: a proteomics study of shell matrix proteins. *ACS Biomater. Sci. Eng.* **5**, 519–529. doi:10.1021/acsbmaterials.8b01355
- Cho, S.-M. and Jeong, W.-G. (2011). Prismatic shell repairs by hemocytes in the extrapallial fluid of the Pacific oyster, *Crassostrea gigas*. *Korean J. Malacol.* **27**, 223–228. doi:10.9710/kjm.2011.27.3.223
- Crane, R. L. and Denny, M. W. (2020). Mechanical fatigue fractures bivalve shells. *J. Exp. Biol.* **223**, jeb220277. doi:10.1242/jeb.220277
- Crane, R. L., Diaz Reyes, J. L. and Denny, M. W. (2021). Bivalves rapidly repair shells damaged by fatigue and bolster strength. *J. Exp. Biol.* **224**, jeb242681. doi:10.1242/jeb.242681
- Crofts, S. B. and Summers, A. P. (2014). How to best smash a snail: the effect of tooth shape on crushing load. *J. R. Soc. Interface* **11**, 20131053. doi:10.1098/rsif.2013.1053
- Currey, J. D. (2002). *Bones: Structure and Mechanics*. Princeton, NJ: Princeton University Press.
- Currey, J. D. and Brear, K. (1984). Fatigue fracture of mother-of-pearl and its significance for predatory techniques. *J. Zool.* **204**, 541–548. doi:10.1111/j.1469-7798.1984.tb02348.x
- Fitzer, S. C., Vittit, L., Bowman, A., Kamenos, N. A., Phoenix, V. R. and Cusack, M. (2015). Ocean acidification and temperature increase impact mussel shell shape and thickness: problematic for protection? *Ecol. Evol.* **5**, 4875–4884. doi:10.1002/eece3.1756

- Gaylord, B., Hill, T. M., Sanford, E., Lenz, E. A., Jacobs, L. A., Sato, K. N., Russell, A. D. and Hettinger, A. (2011). Functional impacts of ocean acidification in an ecologically critical foundation species. *J. Exp. Biol.* **214**, 2586–2594. doi:10.1242/jeb.055939
- George, M. N., O'Donnell, M. J., Concodello, M. and Carrington, E. (2022). Mussels repair shell damage despite limitations imposed by ocean acidification. *J. Mar. Sci. Eng.* **10**, 359. doi:10.3390/jmse10030359
- Goodman, A. M. and Ennos, A. R. (1996). A comparative study of the response of the roots and shoots of sunflower and maize to mechanical stimulation. *J. Exp. Bot.* **47**, 1499–1507. doi:10.1093/jxb/47.10.1499
- Harper, E. M., Clark, M. S., Hoffman, J. I., Philipp, E. E. R., Peck, L. S. and Morley, S. A. (2012). Iceberg scour and shell damage in the antarctic bivalve *Laternula elliptica*. *PLoS ONE* **7**, e46341. doi:10.1371/journal.pone.0046341
- Jaffe, M. J. (1973). Thigmomorphogenesis: the response of plant growth and development to mechanical stimulation. *Planta* **114**, 143–157. doi:10.1007/BF00387472
- Jaffe, M. J., Telewski, F. W. and Cooke, P. W. (1984). Thigmomorphogenesis: on the mechanical properties of mechanically perturbed bean plants. *Physiol. Plant* **62**, 73–78. doi:10.1111/j.1399-3054.1984.tb05925.x
- LaBarbera, M. and Merz, R. A. (1992). Postmortem changes in strength of gastropod shells: evolutionary implications for hermit crabs, snails, and their mutual predators. *Paleobiology* **18**, 367–377. doi:10.1017/S0094837300010940
- Leonard, G. H., Bertness, M. D. and Yund, P. O. (1999). Crab predation, waterborne cues, and inducible defenses in the blue mussel, *Mytilus edulis*. *Ecology* **80**, 1–14. doi:10.1890/0012-9658(1999)080[0001:CPWCAI]2.0.CO;2
- Mach, K. J., Nelson, D. V. and Denny, M. W. (2007). Techniques for predicting the lifetimes of wave-swept macroalgae: a primer on fracture mechanics and crack growth. *J. Exp. Biol.* **210**, 2213–2230. doi:10.1242/jeb.001560
- Meenakshi, V. R., Blackwelder, P. L. and Wilbur, K. M. (1973). An ultrastructural study of shell regeneration in *Mytilus edulis* (Mollusca: Bivalvia). *J. Zool.* **171**, 475–484. doi:10.1111/j.1469-7998.1973.tb02229.x
- Melzner, F., Stange, P., Trübenbach, K., Thomsen, J., Casties, I., Panknin, U., Gorb, S. N. and Gutowska, M. A. (2011). Food supply and seawater pCO₂ impact calcification and internal shell dissolution in the blue mussel *Mytilus edulis*. *PLoS ONE* **6**, e24223. doi:10.1371/journal.pone.0024223
- Mount, A. S., Wheeler, A. P., Paradkar, R. P. and Snider, D. (2004). Hemocyte-mediated shell mineralization in the eastern oyster. *Science* **304**, 297–300. doi:10.1126/science.1090506
- Moyen, N. E., Somero, G. N. and Denny, M. W. (2020). Mussel acclimatization to high, variable temperatures is lost slowly upon transfer to benign conditions. *J. Exp. Biol.* **223**, jeb222893. doi:10.1242/jeb.222893
- O'Neill, M., Mala, R., Cafiso, D., Bignardi, C. and Taylor, D. (2018). Repair and remodelling in the shells of the limpet *Patella vulgata*. *J. R. Soc. Interface* **15**, 20180299. doi:10.1098/rsif.2018.0299
- Palmer, A. R. (1990). Effect of crab effluent and scent of damaged conspecifics on feeding, growth, and shell morphology of the Atlantic dogwhelk *Nucella lapillus* (L.). *Hydrobiologia* **193**, 155–182. doi:10.1007/BF00028074
- Peck, V. L., Oakes, R. L., Harper, E. M., Manno, C. and Tarling, G. A. (2018). Pteropods counter mechanical damage and dissolution through extensive shell repair. *Nat. Commun.* **9**, 264. doi:10.1038/s41467-017-02692-w
- Richardson, C. A. (1989). An analysis of the microgrowth bands in the shell of the common mussel *Mytilus edulis*. *J. Mar. Biol. Assoc. UK* **69**, 477–491. doi:10.1017/S0025315400029544
- Shanks, A. L. and Wright, W. G. (1986). Adding teeth to wave action: the destructive effects of wave-borne rocks on intertidal organisms. *Oecologia* **69**, 420–428. doi:10.1007/BF00377065
- Sleight, V. A., Thorne, M. A. S., Peck, L. S. and Clark, M. S. (2015). Transcriptomic response to shell damage in the Antarctic clam, *Laternula elliptica*: time scales and spatial localisation. *Mar. Genomics* **20**, 45–55. doi:10.1016/j.margen.2015.01.009
- Stokes, A., Fitter, A. H. and Coutts, M. P. (1995). Responses of young trees to wind and shading: effects on root architecture. *J. Exp. Bot.* **46**, 1139–1146. doi:10.1093/jxb/46.9.1139
- Suresh, S. (1998). *Fatigue of Materials*, 2nd edn. Cambridge: Cambridge University Press.
- Taylor, G. M. (2000). Maximum force production: why are crabs so strong? *Proc. R. Soc. Lond. B Biol. Sci.* **267**, 1475–1480. doi:10.1098/rspb.2000.1167